Journal of Dentistry 147 (2024) 105081

Contents lists available at ScienceDirect

Journal of Dentistry

journal homepage: www.elsevier.com/locate/jdent

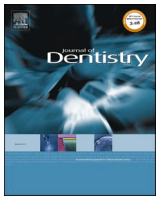

Impact of the superimposition methods on accuracy analyses in complete-arch digital implant investigation

Alvaro Limones [a,*], Rocío Cascos [a], Pedro Molinero-Mourelle [a,b,*], Samir Abou-Ayash [b], Juan Antonio Martínez Vázquez de Parga [a], Alicia Celemin [a,1], Miguel Gómez-Polo [a,1]

[a] Department of Conservative Dentistry and Prosthodontics, Faculty of Odontology, Complutense University of Madrid, Spain
[b] Department of Reconstructive Dentistry and Gerodontology, University of Bern, Bern, Switzerland

ARTICLE INFO

Keywords:
Alignment
Superimposition
Best-fit
Dental implants
Digital dentistry

ABSTRACT

Objectives: To measure the impact of the superimposition methods on accuracy analyses in digital implant research using an ISO-recommended 3-dimensional (3D) metrology-grade inspection software.
Materials and methods: A six-implant edentulous maxillary model was scanned using a desktop scanner (7Series; DentalWings; Montreal, Canada) and an intraoral scanner (TRIOS 4; 3Shape; Copenhagen, Denmark) to generate a reference and an experimental mesh, respectively. Thirty experimental standard tesselletion language (STL) files were superimposed onto the reference model's STL using the core features of six superimposition methods, creating the following groups: initial automated pre-alignment (GI), landmark-based alignment (G1), partial area-based alignment (G2), entire area-based alignment (G3), and double alignment combining landmark-based alignment with entire model area-based alignment (G4) or the scan bodies' surface (G5). The groups underwent various alignment variations, resulting in sixteen subgroups ($n = 30$). The alignment accuracy between experimental and reference meshes was quantified by using the root mean square (RMS) error as trueness and its fluctuation as precision. The Kruskal-Wallis test with a subsequent adjusted post-hoc Dunn's pairwise comparison test was used to analyze the data ($\alpha = 0.05$). The reliability of the measurements was assessed using the intraclass correlation coefficient (ICC).
Results: A total of 480 superimpositions were performed. No significant differences were found in trueness and precision among the groups ($p > 0.05$), except for partial area-based alignment ($p < 0.001$). Subgroup analysis showed significant differences for partial area-based alignment considering only one scan body ($p < 0.001$). Initial automated alignment was as accurate as landmark-based, partial, or entire area-based alignments ($p > 0.05$). Double alignments did not improve alignment accuracy ($p > 0.05$). The entire area-based alignment of the scan bodies' surface had the least effect on accuracy analyses.
Conclusions: Digital oral implant investigation remains unaffected by the superimposition method when ISO-recommended 3D metrology-grade inspection software is used. At least two scan bodies are needed when considering partial area-based alignments.
Clinical significance: The superimposition method choice within the tested ISO-recommended 3D inspection software did not impact accuracy analyses in digital implant investigation.

1. Introduction

A burgeoning wave of scientific research is unfolding within the realm of digital dentistry, with a notable emphasis on the utilization of three-dimensional (3D) inspection software programs. These investigations commonly employ mesh superimposition techniques to meticulously analyze accuracy [1,2]. The analysis process commonly begins with the acquisition of a reference mesh. This process is achieved by scanning a master model using either a desktop or industrial scanner, or alternatively, by directly selecting the digital design created through Computer-Aided Design (CAD) software programs. Subsequently, experimental meshes are generated according to the study's objectives

* Corresponding authors at: Department of Conservative Dentistry and Prosthodontics, Faculty of Odontology, Complutense University of Madrid, Plaza Ramón y Cajal, Madrid 28040, Spain.
E-mail addresses: alimones@ucm.es (A. Limones), pedro.molineromourelle@unibe.ch (P. Molinero-Mourelle).
[1] These authors have contributed equally to this work as senior author.

https://doi.org/10.1016/j.jdent.2024.105081
Received 23 November 2023; Received in revised form 10 May 2024; Accepted 14 May 2024
Available online 24 May 2024

and methodology, i.e. assessing manufacturing accuracy [3,4], studying tooth wear progression [5], appraising intraoral or facial scanner accuracy [6,7], or exploring their influencing factors [8]. Subsequently, these experimental meshes are superimposed on the reference mesh for evaluation purposes. Traditionally, the scientific literature has delineated three primary methods for aligning meshes: landmark-based alignment, partial area-based alignment, and entire area-based alignment [9,10]. Landmark-based and partial area-based alignments hinge on the operator's skills and comprehension of mesh superimposition methods since they require manual selection of common landmarks/points or partial areas [11]. Conversely, area-based alignments merge two-point clouds automatically by iteratively minimizing metric errors through the Gaussian best-fit algorithm, commonly known as the 'Iterative Closest Point' (ICP) algorithm [12]. In digital oral implant investigations, these superimposition methods are commonly used to evaluate the 3D implant position either by employing the root mean square (RMS) error disparity calculation method, or by examining linear and/or angular implant deviation [13-16]. Nevertheless, significant methodological heterogeneity has been observed among similar studies [7,15,17]. At the present time, it remains uncertain if the 3D analysis software choice [18-20], or the specific mesh superimposition methods selected may influence the accuracy measurements [6,10,19,21].

Hence, the primary objective of the present study was to measure the impact of the superimposition method on digital oral implant investigations accuracy analyses. The null hypothesis was that no substantial accuracy differences would exist among the mesh superimposition methods examined. The secondary objectives of this study were:

1. Measure the accuracy of initial pre-alignments.
2. Measure the impact of the spacing or quantity of landmarks on landmark-based alignments.
3. Measure the impact of the size or location of the selected area on partial area-based alignments.
4. Measure the accuracy of double alignments compared to single alignments.
5. Measure the impact of solely employing the region of interest (scan bodies) for the alignment, with a particular emphasis on contrasting the entire area-based alignment of the scan bodies' surface against that based on the attached gingiva, and the combination of both.

2. Materials and methods

The present comparative in vitro study was performed at the Complutense University of Madrid, Spain, and the University of Bern, Switzerland. Ethics approval was not required from the Research Ethics Committee for this in vitro study since no human samples were used.

2.1. Reference model preparation and digitization

A prefabricated maxillary edentulous acrylic resin model (U007A and l-004; Bonemodels, Castellón, Spain) with a 3-mm artificial gingival layer (ST-005 Soft tissue blanket; Bonemodels, Castellón, Spain) to simulate realistic gum tissue was used to mimic the oral environment. Six internal conical connection dental implants (4 mm diameter, 11.5 mm lenght) were equi-crestallly inserted (Ocean; Avinent Implant System, Santpedor, Barcelona, Spain) at the lateral incisors, first premolars, and first molars sites with a 3 mm subgingival positioning. The implants placed at premolar and molar sites were parallel (up to 5° of angulation), and those placed at lateral incisor sites were at a 15-degree angle following the model's anatomy. A 3-mm straight transepithelial implant multi-unit abutment (Abutment Uniblock 3 mm; Avinent Implant System, Santpedor, Barcelona, Spain) was placed on each implant and tightened at 35 Ncm torque by using a calibrated manual torque wrench (Torque wrench; Avinent Implant System, Santpedor, Barcelona, Spain) following the manufacturer's guidelines. In each implant a brand-new scan body (Core Scanbody Transepithelial 1811; Core 3D centers, Santpedor, Spain) was screwed at the implant abutment at 10 Ncm with the same torque wrench. Notably, the implant scan body's bevel feature was oriented towards the lingual surface, a detail according to Gómez-Polo, Álvarez et al., 2022 [17]. All the scan bodies' positions remained stable without any contact until all data acquisition procedures were finalized. For the reference implant casts digitization, a desktop laboratory scanner (7Series Desktop Scanner; Dentalwings, Montréal, Canada) calibrated as per manufacturer's instructions was utilized. The obtained reference scan and the control scan were exported in a standard tessellation language (STL) file format.

2.2. Digital impressions with IOS

The same maxillary model was scanned using an intraoral scanner (IOS) (Trios 4; 3Shape A/S, Copenhagen, Denmark). The IOS was previously calibrated according the manufacturer's recommended protocol [21]. To ensure consistent lighting conditions at 1000 lux, the data collection was performed in a windowless room [22-25], using a light-emitting diode (LED) panel light (660 Pro-RGB; Neewer; Shenzhen; China). The light intensity was measured using a luxmeter (specifically the LX1330B Light Meter; Dr. Meter Digital Illuminance, Union City, USA). All intraoral digital scans were conducted by the same experienced operator (M.G-P) with 7 years of prior experience working with IOSs. The scanning procedure started at the occlusal surface of the scan body of the right first molar. It traversed all occlusal surfaces along the path until reaching the scan body of the contralateral implant. Subsequently, the scanner's orientation was altered to capture the lingual surfaces, starting from the scan body of the left first molar and extending to the right. Then, the process was repeated on the buccal side in the opposite direction to complete the scan, including the palatal rugae. The scans were carefully inspected to ensure their accurate and satisfactory registration. This procedure was repeated to capture 30 specimens, which were then exported in an STL file format.

2.3. Superimposition methods

Utilizing 3D inspection software (Geomagic Control X, 3D Systems, Rock Hill, South Carolina, USA), the 30 IOS STL files were superimposed onto the reference model's STL through six distinct alignment methods, resulting in the following groups:

· An initial automated pre-alignment group (GI).
· A landmark-based alignment group (G1).
· A partial area-based alignment group (G2).
· An entire area-based alignment group (G3).
· A two-stage double combined alignment group consisting of a primary landmark-based alignment followed by a secondary entire area-based alignment of the scan bodies and the attached gingiva (G4).
· A two-stage double combined alignment group consisting of a primary landmark-based alignment followed by a secondary entire area-based alignment of the scan bodies' surface, excluding the gingiva (G5).

The superimposition methods were preceded by an initial automated pre-alignment set by the software. All area-based alignments relied on the Gaussian best-fit algorithm, also known as the "Iterative Closest Point" (ICP) algorithm, which incorporates all surface points and minimizes the mesh distance error to a corresponding data point on the fitting element.

2.4. Accuracy evaluation

To conduct a more comprehensive evaluation of landmark-based alignments (Group 1), sub-analyses were performed to investigate two

factors: the distance between points and the quantity of points. Three subgroups underwent analysis with the aim of assessing whether alterations in the distance between point placements or the number of points could influence the accuracy of the landmark-based alignment:

· Subgroup G1A (Fig. 1.1a) thus utilized three closely positioned points.
· Subgroup G1B (Fig. 1.1b) involved three points widely separated from each other.
· Subgroup G1C (Fig. 1.1c) utilized six points across each scan body (Subgroup G1c; Fig. 1.1c) placed at the mesial vertex of the scan body's flat surface.

To conduct a more thorough evaluation of partial area-based alignments (Group 2), sub-analyses were employed to investigate two factors: the designated area size and its location. Three subgroups underwent analysis with the objective of determining whether adjustments in the area size, corresponding to 1 or 2 scan bodies, or variations in their location, could potentially impact the accuracy of partial area-based alignments:

· Subgroup G2A (Fig. 1.2a) focused on the area of a single scan body.
· Subgroup G2B (Fig. 1.2b) encompassed multiple partial areas by taking two adjacent scan bodies.
· Subgroup G2C (Fig. 1.2c) encompassed multiple partial areas by taking two most distant scan bodies.

For a more in-depth evaluation of the entire area-based alignment, sub-analyses were implemented to explore the implications of solely utilizing the region of interest for the alignment (scan bodies), the attached gingiva, or their combination:

· Subgroup G3A (Fig. 1.3a) focused on both the scan bodies' surface and the immobile attached gingiva.
· Subgroup G3B (Fig. 1.3b) encompassed only the scan bodies' surface for the alignment.
· Subgroup G3C (Fig. 1.3c) encompassed the immobile attached gingiva and the anterior palate for the alignment.

For a comprehensive assessment of double alignments in two-steps, the present study explored the initial application of landmark-based alignments (same for subgroups G1A to G1C) in a first step, followed by a second alignment based on an entire area-based alignment of the scan bodies' surface and the immobile attached gingiva (G4) or the scan bodies' surface only (G5) in a second step (G5). The rationale behind this assessment was to assess whether double alignments show any substantial accuracy differences compared to single alignments. Consequently, six subgroups were established:

· Subgroup G4A (Fig. 1.4a) employed a primary landmark-based alignment using three closely positioned points, followed by a secondary entire area-based alignment of both the scan bodies' surface and the immobile attached gingiva.
· Subgroup G4B (Fig. 1.4b) employed a primary landmark-based alignment using three widely separated points, followed by a secondary entire area-based alignment of both the scan bodies' surface and the immobile attached gingiva.
· Subgroup G4C (Fig. 1.4c) employed a primary landmark-based alignment using six points across each scan body placed at the mesial vertex of the scan body's flat surface, followed by a secondary entire area-based alignment of both the scan bodies' surface and the immobile attached gingiva.
· Subgroup G5A (Fig. 1.5a), employed a primary landmark-based alignment using three closely positioned points, followed by a secondary entire area-based alignment of the scan bodies' surface.
· Subgroup G5B (Fig. 1.5b) employed a primary landmark-based alignment using three widely separated points, followed by a secondary entire area-based alignment of the scan bodies' surface.
· Subgroup G5C (Fig. 1.5c) employed a primary landmark-based alignment using six points across each scan body placed at the mesial vertex of the scan body's flat surface, followed by a secondary entire area-based alignment of the scan bodies' surface.

2.5. Sample size calculation

The sample size calculation was conducted based on the study of Revilla-León, Gohil et al. in 2023 [21]. The study aimed to detect a difference in trueness (primary outcome) of 10±13.5 μm between landmark-based and entire area-based alignment. The calculation employed a 1:1 sampling ratio, a significance level (alpha) of 5 %, 90 % statistical power, and a two-sided paired-mean hypothesis test. The determined suitable sample size for each alignment group was 28 specimens. However, to account for potential sample loss due to artifacts that could compromise the analysis and unforeseen issues, a total of 30 STL files per subgroup was selected as the final sample size.

2.6. Outcome measures

The primary outcome of this in vitro study was to assess the accuracy by trueness and precision in microns (μm). Trueness was defined as the average RMS error discrepancies on the superimposition of the reference and experimental scans (ISO 5725-1:1994; ISO 20896-1:2019) [26,27]. Precision was detailed as the RMS error fluctuations per each group or standard deviation (SD) (ISO 5725-1:1994; ISO 20896-1:2019) [26,27]. The calculation of RMS error was performed considering the scan bodies' surface solely (Fig. 2) and using the following formulae $RMS = \sqrt{\frac{\sum_{i=1}^{n}\left(X_{1,i}-X_{2,j}\right)^2}{n}}$ where $X_{1,i}$ are the reference data, $X_{2,j}$ are the scan data, and n indicated the total number of measurement points analyzed in each examination. The discrepancies calculations for each group were employed for data analysis.

2.7. Statistical analysis

Independent blinded statistical analyses were performed using a coded default Excel spreadsheet to ensure the prevention of data manipulation or hypothesis testing. After the statistical analysis, the coding was revealed to edit tables and graphs. The results of the Shapiro–Wilk tests indicate that the trueness and precision data exhibited a non-normal distribution ($p < 0.05$). Consequently, the Kruskal-Wallis test with a subsequent adjusted post hoc Dunn's pairwise comparisons test was used to assess the influence of the superimposition methods on trueness and precision at both the group and subgroup levels. The operator's measurement reliability was evaluated using the intraclass correlation coefficient (ICC). Data analysis and visualization were conducted utilizing the statistical software program STATA (v 17.0; StataCorp LP, TX, USA).

3. Results

A total of 480 superimpositions constituted the study sample, which belonged to 6 groups categorized into 16 subgroups. Table 1 and Fig. 3 show the trueness and precision values obtained from the tested subgroups. The ICC for assessing the operator's reliability was 0.78 (95 % CI: 0.65–0.90), indicating good intra-examiner consistency.

Concerning trueness, the Kruskal-Wallis test yielded statistically significant variance in trueness values among the evaluated groups ($p < 0.001$). Further post-hoc analysis using Dunn's test indicated notable trueness differences between the G2 and other superimposition groups

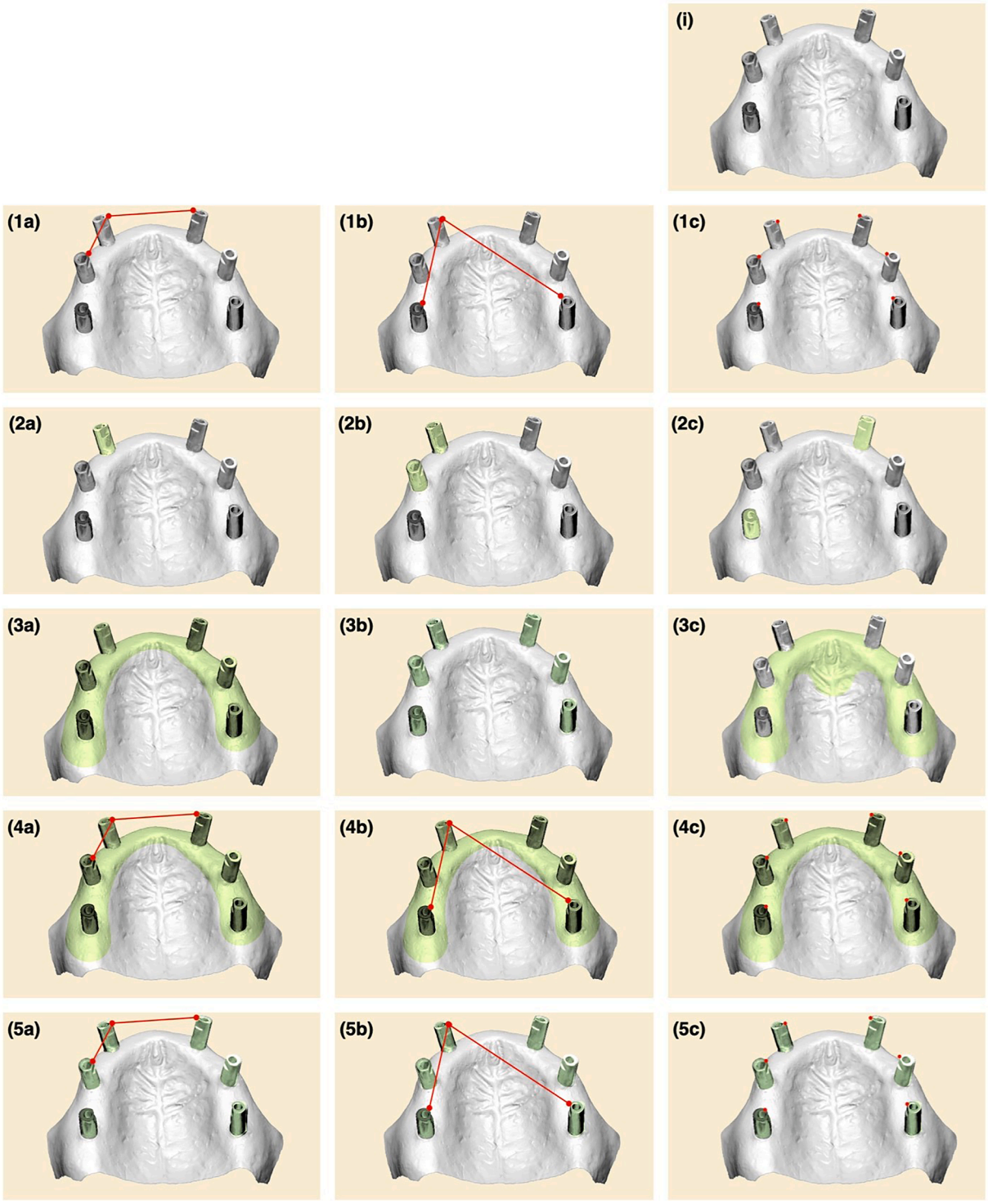

Fig. 1. Superimposition methods tested: (i) Initial automated pre-alignment; (1a) 3 close-point landmark-based alignment; (1b) 3 distant-point landmark-based alignment; (1c) 6-point landmark-based alignment; (2a) partial area-based alignment of one scan body's surface; (2b) partial area-based alignment of two-close scan bodies' surface; (2c) partial area-based alignment of two-distant scan bodies' surface; (3a) entire area-based alignment; (3b) entire area-based alignment of the scan bodies' surface; (3c) entire area-based alignment of the immobile attached gingiva solely ; (4a) primary 3 close-point landmark-based alignment followed by a secondary entire area-based alignment; (4b) primary 3 distant-point landmark-based alignment followed by a secondary entire area-based alignment; (4c) primary 6-points landmark-based alignment followed by a secondary entire area-based alignment; (5a) primary 3 close-point landmark-based alignment followed by a secondary entire area-based alignment of the scan bodies' surface; (5b) primary 3 distant-point landmark-based alignment followed by a secondary entire area-based alignment of the scan bodies' surface; (5c) primary 6-points landmark-based alignment followed by a secondary entire area-based alignment of the scan bodies' surface.

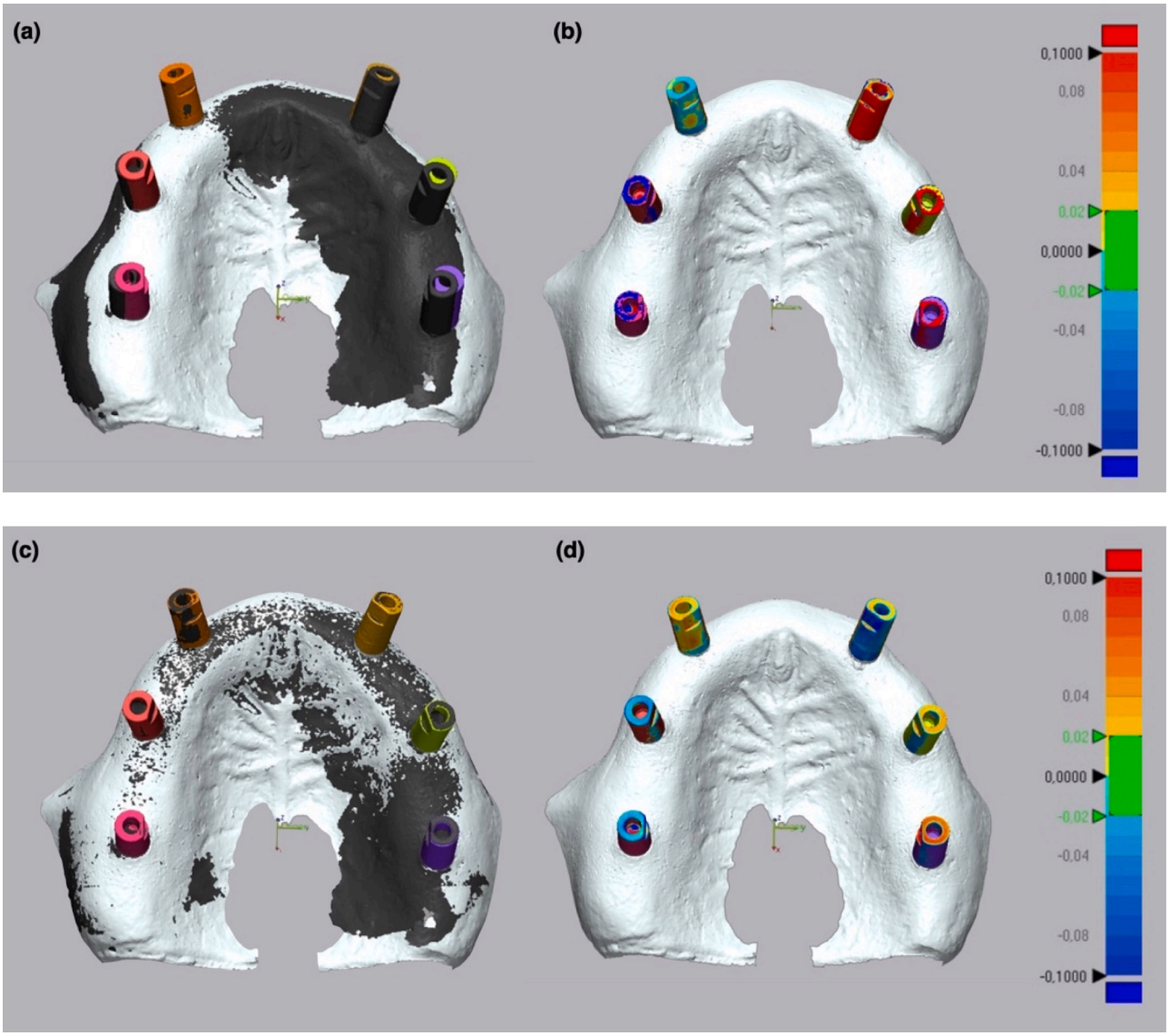

Fig. 2. (a) Representation of a IOS STL file superimposed onto the reference model's STL using a partial area-based alignment of one scan body's surface. (b) Representative color map of the RMS error discrepancies measured when a partial area-based alignment of one scan body's surface was used. (c) Representation of a IOS STL file superimposed onto the reference model's STL using the entire area-based alignment of the scan bodies' surface. (d) Representative color map of the RMS error discrepancies measured when the entire area-based alignment of the scan bodies' surface was used.

($p < 0.001$). Specifically, upon subgroup analysis, the G2a subgroup was found to significantly contribute to this trueness distinction ($p < 0.001$). However, no other superimposition methods exhibited significant trueness discrepancies.

Regarding precision, the Kruskal-Wallis test demonstrated statistically significant variability in the precision values among the assessed groups ($p < 0.001$). Subsequent post-hoc analysis utilizing Dunn's test revealed significant precision disparities between the G2 and the remaining superimposition groups ($p < 0.001$). Upon closer examination through subgroup analysis, it was identified that the G2a subgroup played a substantial role in driving this precision differentiation ($p < 0.001$). Nevertheless, no other superimposition methods exhibited significant precision discrepancies.

4. Discussion

The present investigation revealed that mesh superposition methods had a limited impact on the accuracy analyses of digital oral implant research. No alignment method, including the inspection program's initial pre-alignment, found significant differences in trueness and precision values, except for the partial area-based alignment. Considering these differences, the study's null hypothesis was partially confirmed. According to a subgroup analysis, these disparities were caused by the subgroup that focused exclusively on the surface of a single scan body, indicating that the size and the number of the selected areas can indeed impact accuracy, specially when a unique and reduced area is involved. The location of the chosen scan bodies did not significantly impact the accuracy. The points increasing or their spatial separation did not yield accuracy enhancements, nor the utilization of double.

The most accurate superimposition fit was achieved through the entire area-based alignment of the scan bodies' surface, with a value of 95±48 μm. This could be attributed to the standardized geometry of scan bodies, making them easier to accurately align [19] or to the fact that the entire area-based alignment method eliminates operator-based decisions, contrasting with landmark-based or partial area-based alignments.

In partial area-based alignment, the higher discrepancy was caused by the unilateral selection of one scan body surface. These findings

Table 1
Median ± IQR values of trueness and precision calculated for each superposition method and organized in descending order according to their influence on accuracy. Identical superscripts indicate statistically significant differences among subgroups.

Subgroup	N	Trueness (μm)			Precision (μm)		
		Median	±	IQR	Median	±	IQR
G3b	30	95[a]	±	58	91[a']	±	57
G5a	30	95[b]	±	58	91[b']	±	57
G5b	30	95[c]	±	58	91[c']	±	57
G5c	30	95[d]	±	58	91[d']	±	57
Inicial	30	99[e]	±	56	97[e']	±	56
G1a	30	99[f]	±	56	97[f']	±	56
G1b	30	99[g]	±	56	97[g']	±	56
G1c	30	99[h]	±	56	97[h']	±	56
G3a	30	104[i]	±	58	102[i']	±	53
G4a	30	104[j]	±	58	102[j']	±	53
G4b	30	104[k]	±	58	102[k']	±	53
G4c	30	104[l]	±	58	102[l']	±	53
G3c	30	107[m]	±	55	105[m']	±	52
G2c	30	118[n]	±	65	117[n']	±	60
G2b	30	143[o]	±	68	138[o']	±	66
G2a	30	515[a-o]	±	208	515[a'-o']	±	205

aligned with those of prior studies that evaluated the same interventions under similar conditions in dentate models [28]. Moreover, these results were consistent with the color maps, revealing a heterogeneous deviation pattern with more red areas on the implants opposite to the scan body surface used for alignment indicating outward deviations. Conversely, green, or yellow areas show deviations within the tolerance range, or slight outward deviations were observed on the scan body used for alignment. However, when the surfaces of two scan bodies were used for alignment, similar accuracy values were obtained as compared to the rest of superimposition methods.

In contrast with the present study, prior in vitro studies reported that partial area-based alignment achieved the highest level of alignment accuracy on facial and intraoral dentate scans [6,21]. This may be attributed to the fact that the study of Revilla-León et al., adopted a multiple partial areas approach for the partial area-based alignment, which differs from our study's on the consideration of one or maximum two scan bodies surfaces for the partial area-based alignment.

The inherent potential of this alignment is to prevent superimposition errors when the experimental mesh contains artifacts. This becomes particularly significant in clinical scenarios where digital impressions extend beyond the immobile attached gingiva or involve incorrect scanning patterns. Consequently, adopting a superimposition strategy based on points or partial areas free from artifacts could offer a more precise and reliable fit, despite the subjective nature of these methods.

Peroz et al., explored various alignment algorithms, including the Gauss best-fit algorithm and the exterior, median, or interior Chebyshev best-fit algorithm [19]. However, the aim of the study was not to assess the complex internal algorithms of each software, as our study specifically employed the Gauss best-fit algorithm for all area-based alignments. Nevertheless, this might be an additional factor to consider as different 3D inspection software may produce different measurements

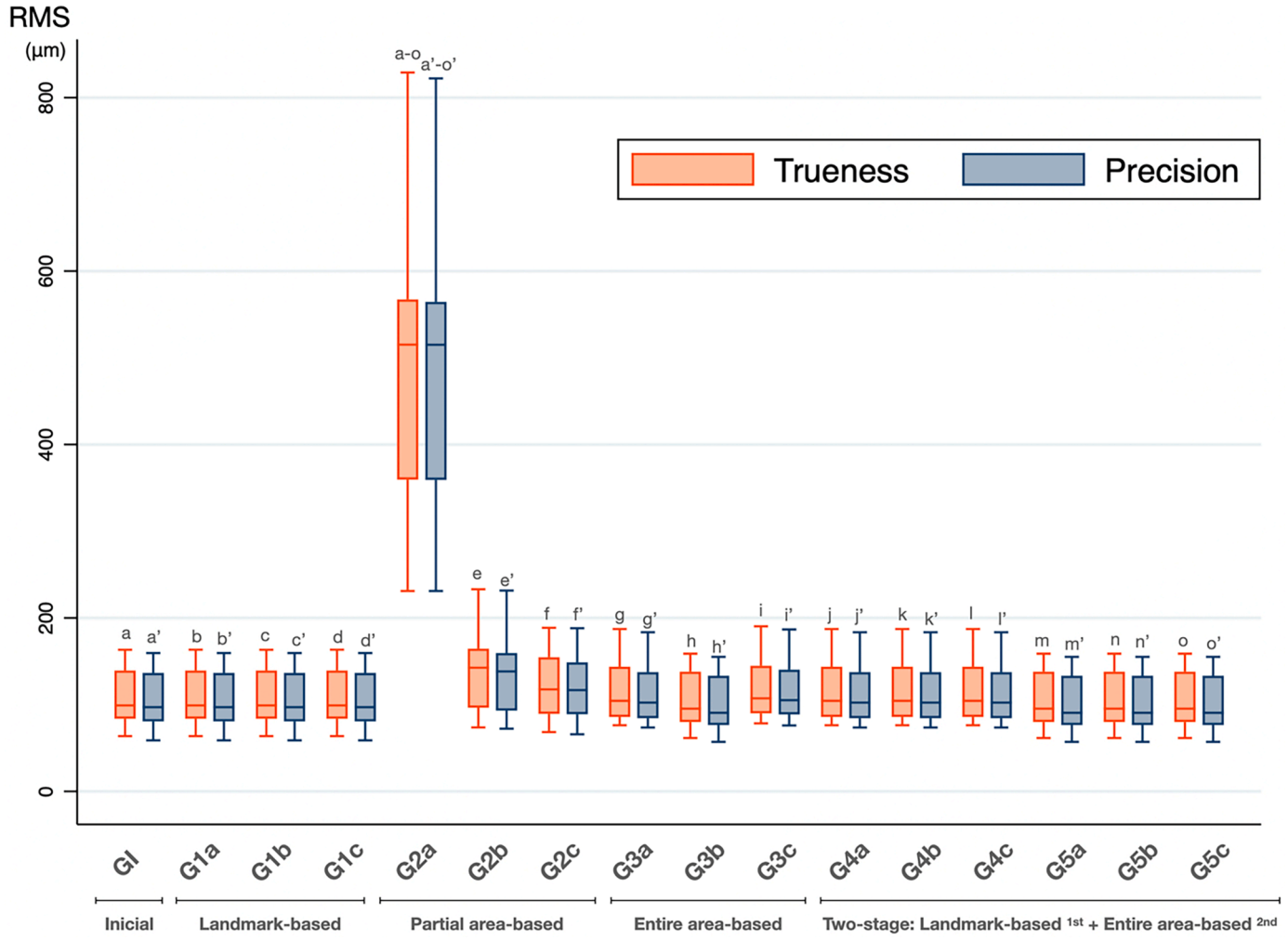

Fig. 3. Accuracy analysis – Box plot graph of trueness and precision values by subgroup.

[18-20]. In the present study, ISO-recommended metrology-grade software was employed by using the RMS method. Different results may be obtained if different deviation measurement instruments are used [18]. Various deviation measurement methods may yield different results [18]. Hence, in future studies, it would be beneficial to explore further additional softwares, such as other metrology-grade options, as well as non-metrology-grade freeware programs.

The clinical significance of this study lies in how superimposition methods affect accuracy analyses in digital implantology investigations. Furthermore, it offers valuable insights against the inefficiency of double alignments, excessive point marking, or relying on a single scan body for alignment. Therefore, these findings can guide future research in this field. Potential future research avenues might involve exploring reverse (extraoral) scan-body methodologies for previously crafted complete-arch fixed dental prostheses (FDPs), as well as for angulated implants or mandibular models.

The present research has several limitations, including the examination of a single inspection software and the exclusive focus on a maxillary. Different inspection software programs could potentially yield different outcomes. Furthermore, a noteworthy aspect missing from the study is the contemplation of implant angulation.

5. Conclusions

The measured accuracy in digital implant investigations remains unaffected by the superimposition method used in the tested 3D inspection software, except when the alignment relies on a unique scan body area. A minimum of two independent scan body surfaces is required when considering a partial area-based alignment. Besides, the findings show critical insights for future research, especially in considering the following practical implications for accuracy evaluation.

5.1 Automated initial pre-alignments exhibited comparable accuracy in comparison to other superimposition methods.
5.2 Increasing the quantity of points or modifying their spatial distribution in landmark-based alignments did not result in improved accuracy.
5.3 Adjusting the size or position of a specific partial area on one side in the partial area-based alignment did not yield accuracy improvements.
5.4 Double mesh superimposition method did not show accuracy improvements.
5.5 The exclusive selection of the area of interest (scan bodies) for alignment did not prove to be more accurate than other superimposition methods.

Funding information

Not applicable.

Ethics approval statement

This in vitro study was exempt from ethics committee approval.

CRediT authorship contribution statement

Alvaro Limones: Formal analysis, Methodology, Project administration, Visualization, Writing – review & editing, Writing – original draft, Conceptualization. **Rocío Cascos:** Software, Data curation. **Pedro Molinero-Mourelle:** Writing – review & editing, Writing – original draft, Data curation. **Samir Abou-Ayash:** Writing – review & editing, Writing – original draft, Supervision. **Juan Antonio Martínez Vázquez de Parga:** Writing – review & editing, Supervision, Formal analysis. **Alicia Celemin:** Writing – review & editing, Supervision, Formal analysis, Conceptualization. **Miguel Gómez-Polo:** Writing – review & editing, Supervision, Data curation.

Declaration of competing interest

The authors have no conflict of interest to report pertaining to the conduction of this study.

Data availability

The data that support the findings of this study are available from the corresponding author upon reasonable request.

References

[1] T. Joda, U. Brägger, G. Gallucci, Systematic literature review of digital three-dimensional superimposition techniques to create virtual dental patients, Int. J. Oral Maxillofac. Implant. 30 (2) (2015) 330–337, https://doi.org/10.11607/jomi.3852.
[2] H. Yilmaz, H. Arınç, G. Çakmak, S. Atalay, M.B. Donmez, A.M. Kökat, B. Yilmaz, Effect of scan pattern on the scan accuracy of a combined healing abutment scan body system, J. Prosthet. Dent. 131 (1) (2024) 110–118, https://doi.org/10.1016/j.prosdent.2022.01.018.
[3] H. Lerner, K. Nagy, N. Pranno, F. Zarone, O. Admakin, F. Mangano, Trueness and precision of 3D-printed versus milled monolithic zirconia crowns: an in vitro study, J. Dent. 113 (2021) 103792, https://doi.org/10.1016/j.jdent.2021.103792.
[4] G. Çakmak, A.M. Rusa, M.B. Donmez, C. Akay, Ç. Kahveci, M. Schimmel, B. Yilmaz, Trueness of crowns fabricated by using additively and subtractively manufactured resin-based CAD-CAM materials, J. Prosthet. Dent. 131 (5) (2024) 951–958, https://doi.org/10.1016/j.prosdent.2022.10.01.
[5] C. Wulfman, V. Koenig, A. Mainjot, Wear measurement of dental tissues and materials in clinical studies: a systematic review, Dent. Mater. 34 (6) (2018) 825–850, https://doi.org/10.1016/j.dental.2018.03.002.
[6] M. Revilla-León, J.A. Pérez-Barquero, B.A. Barmak, R. Agustín-Panadero, L. Fernández-Estevan, W. Att, Facial scanning accuracy depending on the alignment algorithm and digitized surface area location: an in vitro study, J. Dent. 110 (2021) 103680, https://doi.org/10.1016/j.jdent.2021.103680.
[7] V. Vitai, A. Németh, E. Sólyom, L.M. Czumbel, B. Szabó, R. Fazekas, G. Gerber, P. Hegyi, P. Hermann, J. Borbély, Evaluation of the accuracy of intraoral scanners for complete-arch scanning: a systematic review and network meta-analysis, J. Dent. 137 (2023) 104636, https://doi.org/10.1016/j.jdent.2023.104636.
[8] A.L.C. Pereira, M.R.S. Curinga, H.V.M. Segundo, A.d.F.P. Carreiro, Factors that influence the accuracy of intraoral scanning of total edentulous arches rehabilitated with multiple implants: a systematic review, J. Prosthet. Dent. 129 (6) (2023) 855–862, https://doi.org/10.1016/j.prosdent.2021.09.001.
[9] H. Mora, J.M. Mora-Pascual, A. Garcia-Garcia, P. Martinez-Gonzalez, Computational analysis of distance operators for the iterative closest point algorithm, PLoS One 11 (10) (2016) e0164694, https://doi.org/10.1371/journal.pone.0164694.
[10] S. O'Toole, C. Osnes, D. Bartlett, A. Keeling, Investigation into the accuracy and measurement methods of sequential 3D dental scan alignment, Dent. Mater. 35 (3) (2019) 495–500, https://doi.org/10.1016/j.dental.2019.01.012.
[11] K. Becker, B. Wilmes, C. Grandjean, D. Drescher, Impact of manual control point selection accuracy on automated surface matching of digital dental models, Clin. Oral Investig. 22 (2) (2018) 801–810, https://doi.org/10.1007/s00784-017-2155-6.
[12] S. Rusinkiewicz, M. Levoy, Efficient variants of the ICP algorithm, in: Proceedings third international conference on 3-D digital imaging and modeling, IEEE, 2001, pp. 145–152.
[13] S. Rothlauf, S. Pieralli, C. Wesemann, F. Burkhardt, K. Vach, F. Kernen, B.C. Spies, Influence of planning software and template design on the accuracy of static computer assisted implant surgery performed using guides fabricated with material extrusion technology: an in vitro study, J. Dent. 132 (2023) 104482, https://doi.org/10.1016/j.jdent.2023.104482.
[14] N. Tahir, J. Abduo, An in vitro evaluation of the effect of 3d printing orientation on the accuracy of implant surgical templates fabricated by desktop printer, J. Prosthodont. 31 (9) (2022) 791–798, https://doi.org/10.1111/jopr.13485.
[15] A. Sallorenzo, M. Gómez-Polo, Comparative study of the accuracy of an implant intraoral scanner and that of a conventional intraoral scanner for complete-arch fixed dental prostheses, J. Prosthet. Dent. 128 (5) (2022) 1009–1016, https://doi.org/10.1016/j.prosdent.2021.01.032.
[16] M. Gómez-Polo, R. Ortega, A. Sallorenzo, R. Agustín-Panadero, A.B. Barmak, J. C. Kois, M. Revilla-León, Influence of the surface humidity, implant angulation, and interimplant distance on the accuracy and scanning time of complete-arch implant scans, J. Dent. 127 (2022) 104307, https://doi.org/10.1016/j.jdent.2022.104307.
[17] M. Gómez-Polo, F. Álvarez, R. Ortega, C. Gómez-Polo, A.B. Barmak, J.C. Kois, M. Revilla-León, Influence of the implant scan body bevel location, implant angulation and position on intraoral scanning accuracy: an in vitro study, J. Dent. 121 (2022) 104122, https://doi.org/10.1016/j.jdent.2022.104122.
[18] B. Yilmaz, V.R. Marques, M.B. Donmez, A.R. Cuellar, W.-E. Lu, S. Abou-Ayash, G. Çakmak, Influence of 3D analysis software on measured deviations of CAD-CAM resin crowns from virtual design file: an in-vitro study, J. Dent. 118 (2022) 103933, https://doi.org/10.1016/j.jdent.2021.103933.

[19] S. Peroz, B.C. Spies, U. Adali, F. Beuer, C. Wesemann, Measured accuracy of intraoral scanners is highly dependent on methodical factors, J. Prosthodont. Res. 66 (2) (2022) 318–325, https://doi.org/10.2186/jpr.JPR_D_21_00023.
[20] K. Son, W.-S. Lee, K.-B. Lee, Effect of different software programs on the accuracy of dental scanner using three-dimensional analysis, Int. J. Environ. Res. Public Health 18 (16) (2021) 8449, https://doi.org/10.3390/ijerph18168449.
[21] M. Revilla-León, A. Gohil, A.B. Barmak, A. Zandinejad, A.J. Raigrodski, J.A. Pérez-Barquero, Best-fit algorithm influences on virtual casts' alignment discrepancies, J. Prosthodont. 32 (4) (2023) 331–339, https://doi.org/10.1111/jopr.13537.
[22] M. Revilla-León, P. Jiang, M. Sadeghpour, W. Piedra-Cascón, A. Zandinejad, M. Özcan, V.R. Krishnamurthy, Intraoral digital scans—Part 1: influence of ambient scanning light conditions on the accuracy (trueness and precision) of different intraoral scanners, J. Prosthet. Dent. 124 (3) (2020) 372–378, https://doi.org/10.1016/j.prosdent.2019.06.003.
[23] M. Revilla-León, P. Jiang, M. Sadeghpour, W. Piedra-Cascón, A. Zandinejad, M. Özcan, V.R. Krishnamurthy, Intraoral digital scans: part 2—influence of ambient scanning light conditions on the mesh quality of different intraoral scanners, J. Prosthet. Dent. 124 (5) (2020) 575–580, https://doi.org/10.1016/j.prosdent.2019.06.004.
[24] M. Revilla-León, S.G. Subramanian, M. Özcan, V.R. Krishnamurthy, Clinical study of the influence of ambient light scanning conditions on the accuracy (trueness and precision) of an intraoral scanner, J. Prosthodont. 29 (2) (2020) 107–113, https://doi.org/10.1111/jopr.13135.
[25] M. Revilla-León, S.G. Subramanian, W. Att, V.R. Krishnamurthy, Analysis of different illuminance of the room lighting condition on the accuracy (trueness and precision) of an intraoral scanner, J. Prosthodont. 30 (2) (2021) 157–162, https://doi.org/10.1111/jopr.13276.
[26] International Organization for Standardization, ISO 5725-1:1994Accuracy (trueness and precision) of Measurement Methods And Results— Part 1: General Principles and Definitions, 1994. Retrieved January 2, 2020, from, https://www.iso.org/obp/ui/#iso:std:iso:5725:-1:ed-1:v1:en.
[27] International Organization for Standardization, ISO 20896-1:2019. Dentistry—Digital Impression Devices—Part 1: Methods for Assessing Accuracy, 2019. Retrieved January 2, 2020, from, https://www.iso.org/standard/69402.html.
[28] A. Limones, P. Molinero-Mourelle, G. Çakmak, S. Abou-Ayash, S. Delgado, J. A. Martínez Vázquez de Parga, A. Celemín, Impact of the superimposition methods and the designated comparison area on accuracy analyses in dentate models, J. Dent. 145 (2024) 104939, https://doi.org/10.1016/j.jdent.2024.104939.